Astron. Astrophys. 356, 363–372 (2000)

ASTRONOMY AND ASTROPHYSICS

New solution to viscous evolution of accretion disks in binary systems

G.V. Lipunova[1] **and N.I. Shakura**[1,2]

[1] Sternberg Astronomical Institute, Moscow State University, Universitetskii pr. 13, Moscow, 119899 Russia
[2] Max-Planck-Institut für Astrophysik, Karl-Schwarzschild-Str. 1, D-85740 Garching, Germany

Received 31 May 1999 / Accepted 11 January 2000

Abstract. The analytical investigation of time-dependent accretion in disks is carried out. We consider a time-dependent disk in a binary system at outburst which has a fixed tidally-truncated outer radius. The standard model (Shakura-Sunyaev) of the disk is considered. The vertical structure of the disk is accurately described in two regimes of opacity: Thomson and free-free. The fully analytical solutions are obtained, characterized by power-law variations of accretion rate with time. The solutions supply asymptotic description of the disk evolution in flaring sources in the periods after outbursts while the disk is fully ionized. The X-ray flux of multicolor (black-body) α-disk is obtained as varying quasi-exponentially. The application to X-ray novae is briefly discussed concerning the observed faster-than-power decays of X-ray light curves. The case of time-dependent advective disk when the exponential variations of accretion rate can occur is discussed.

Key words: accretion, accretion disks – stars: binaries: close – stars: novae, cataclysmic variables – X-rays: bursts

1. Introduction

We investigate analytically the problem of time-dependent accretion, closely related to the phenomena of flares widely observed in binary systems. In this paper we will concern ourselves with the emission of the flaring source which is generated by the accretion disk. We suppose the light curve to be regulated by the accretion rate variations. Such sources are typified by the low-mass X-ray binaries and cataclysmic variables.

After Weizsäcker (1948) who considered the evolution of a protoplanetary cloud, the analytical investigations of non-stationary accretion were carried out by Lüst (1952), Lynden-Bell & Pringle (1974), Lyubarskii & Shakura (1987, hereafter LS87) as applied to accretion disks. A brief overview is presented in the book by Kato et al. (1998).

LS87 suggested three stages of evolution of a time-dependent accretion disk (see also Sect. 5.1). Initially a finite torus of the increased density is formed around a gravitational centre. Viscosity causes the torus to spread and develop into the disk (1st stage). After the disk approaches the centre, the accretion rate reaches the maximum value (2nd stage) and begins to descend (3rd stage). During this stage the total angular momentum of the disk is conserved.

Ogilvie (1999) presented a time-dependent self-similar analytical solution for a quasi-spherical advection-dominated flow with conserved total angular momentum.

In a binary system, variations of accretion rate can be due to the non-stationary exchange of mass between the components of the binary (mass-overflow instability model) or due to the disk instability processes (see Kato et al. 1998 and references therein). At some time the accretion rate onto the centre begins to augment. We assume that the maximum accretion rate through the inner boundary of the disk corresponds to a peak of outburst and the accretion rate decreases afterwards.

In this study we particularly focus on the stage soon after the outburst. In Sect. 2 we outline the general equations of time-dependent accretion. The basic equation relates surface density of the disk and viscous stresses in it. Thus the specific structure of the disk influences greatly the run of the process. Sect. 3 introduces the investigation of time-dependent Keplerian α-disks. The vertical structure of standard Keplerian disk is considered in Sect. 4. In a binary system the third stage of LS87 cannot be realized because the accretion disk around a primary would be confined by the gravitational influence of a secondary. Such disks do not preserve their angular momentum, transferring it to the orbital motion. We suggest the particular conditions at the outer boundary of the disk which allow the acquisition of new solutions characterized by faster decays than in LS87. The procedure and the analytical solution are presented in Sect. 5.

We calculate the resulting bolometric light curve taking into account the transition between the opacity regimes as accretion rate decreases (Sect. 6). We note that observed light curves can have different slopes due to unevenness of spectral distribution (Sect. 7).

In Sect. 8 we discuss the case of advection-dominated accretion flow (ADAF) in which exponential variations with time of accretion rate possibly take place.

In Sect. 9 we discuss application of our model to X-ray novae.

Send offprint requests to: G.V. Lipunova
Correspondence to: galja@sai.msu.ru

2. Basic non-stationary accretion disk equation

In the approximation of Newtonian potential we assume that the velocity of a free particle orbiting at distance r around a gravitating object is

$$\omega_{\rm K} r = (GM/r)^{1/2} \,, \tag{1}$$

where $\omega_{\rm K}$ is the Kepler angular velocity; M is the mass of the central gravitating object, constant in time; $G = 6.67 \times 10^{-8}$ cm^3 g^{-1} s^{-2} is the gravitational constant. This is a good approximation to the law of motion for particles in the standard sub-Eddington disk. In the advection-dominated accretion flow (ADAF) the particles are substantially subjected to the radial gradient of pressure and thus have the velocity different from that given by (1). Following the model by Narayan & Yi (1994), one can assume that the angular velocity in ADAF is $\omega = c_2\,\omega_{\rm K}$.

The height-integrated Euler equation on φ and the continuity equation along the height Z are given by:

$$\Sigma_{\rm o}\, v_r\, \frac{\partial\,(\omega\, r^2)}{\partial r} = -\,\frac{1}{r}\,\frac{\partial}{\partial r}\,(W_{r\varphi} r^2) \,, \tag{2}$$

$$\frac{\partial \Sigma_{\rm o}}{\partial t} = -\,\frac{1}{r}\,\frac{\partial}{\partial r}\,\Sigma_{\rm o} v_r r \,, \tag{3}$$

where ω is the angular velocity in the disk; $\Sigma_{\rm o}(r,t) = 2\int\limits_0^{Z_{\rm o}} \rho\,{\rm d}Z$ – the surface density of the matter, and $W_{r\varphi}(r,t) = 2\int\limits_0^{Z_{\rm o}} w_{r\varphi}\,{\rm d}Z$ is the height-integrated viscous shear stresses between adjacent layers. The time-independent angular velocity is assumed although there can possibly be certain variations of ω in the non-Keplerian advective disks when a time-dependent pressure gradient is involved (see, e.g. Ogilvie 1999).

It is convenient to introduce the following variables: $F = W_{r\varphi} r^2$, henceforth $2\pi F$ means the total moment of viscous forces acting between the adjacent layers, $h_* = \omega r^2$ – the specific angular momentum of the matter in the disk, and $h \equiv \omega_{\rm K} r^2$. From Eq. (2) in view of (1) it follows that

$$\Sigma_{\rm o}\, v_r\, r \;= \frac{\dot{M}(r,t)}{2\,\pi} = -\left[\frac{\partial h_*}{\partial h}\right]^{-1} \frac{\partial F}{\partial h} \,. \tag{4}$$

Substituting (4) in (3) and expressing r in terms of h, we obtain the basic equation of time-dependent accretion:

$$\frac{\partial \Sigma_{\rm o}}{\partial t} = \frac{1}{2}\,\frac{(GM)^2}{h^3}\,\frac{\partial}{\partial h}\left(\left[\frac{\partial h_*}{\partial h}\right]^{-1}\frac{\partial F}{\partial h}\right) \,. \tag{5}$$

In the case of the Keplerian disk $\partial h_*/\partial h = 1$. The advection-dominated solution by Narayan and Yi (1994) yields $\partial h_*/\partial h = c_2$, where c_2 is a dimensionless constant.

3. Non-linear problem of evolution of the standard Shakura-Sunyaev disk

The special case when the moment of viscous forces depends linearly on the surface density and has a power law dependence on the radius ($F \propto \Sigma_{\rm o} h^l$) was thoroughly investigated by Lynden-Bell & Pringle (1974). In this particular case Eq. (5) is linear and the solution can be presented as the superposition of particular solutions (Green's functions) while the non-linear equations do not allow such solutions. In the paper by LS87 the necessary relation between $\Sigma_{\rm o}$ and F for α-disks (Shakura 1972; Shakura & Sunyaev 1973) was derived from the vertical structure equations. Then Eq. (5) acquires the following non-linear form taking into account that $h \equiv h_*$:

$$\frac{\partial F}{\partial t} = D\,\frac{F^m}{h^n}\,\frac{\partial^2 F}{\partial h^2} \,, \tag{6}$$

where D is the dimension constant; $m = 2/5$, $n = 6/5$ when the Thomson scattering dominates the opacity in the accretion disk, and $m = 3/10$, $n = 4/5$ when the free-free and free-bound transitions do. The "diffusion constant" D, defined by the specific vertical structure, relates $\Sigma_{\rm o}$, F, and h:

$$\Sigma_{\rm o} = \frac{(GM)^2\, F^{1-m}}{2\,(1-m)\,D\,h^{3-n}} \tag{7}$$

(see also Filipov 1984). D is a function of α, opacity coefficient, and the dimensionless values, which are the combinations of the characteristic physical parameters of the disk. The value of D is to be derived from the consideration of the disk vertical structure. In the following section we obtain its value using the results of the work by Ketsaris & Shakura (1998).

4. Vertical structure of standard disk

Hereafter, until specially mentioned, we assume that the matter in the disk moves with the Keplerian angular velocity $\omega_{\rm K}$, and its state is governed by the ideal gas equation

$$P = \frac{\rho\,\Re\,T}{\mu} \,, \tag{8}$$

where μ and $\Re = 8.31 \times 10^7$ erg mol^{-1}K^{-1} are the molecular weight of the gas and the molar gas constant, respectively. Along the Z coordinate the hydrostatic equilibrium takes place:

$$\frac{1}{\rho}\,\frac{\partial P}{\partial Z} = -\omega_{\rm K}^2 Z \tag{9}$$

and the continuity equation is

$$\frac{\partial \Sigma}{\partial Z} = \rho \,. \tag{10}$$

We assume the radiation transfer equation in the diffusive approximation:

$$\frac{c}{3\,\varkappa\,\rho}\,\frac{\partial (aT^4)}{\partial Z} = -\,Q \,, \tag{11}$$

where $c = 2.99 \times 10^{10}$ cm s^{-1} is the light velocity, $a = 7.56 \times 10^{-15}$ erg cm^{-3}K^{-4}. The vertical gradient of the radiation flux Q is proportional to the energy release per unit volume in the disk; that is,

$$\frac{\partial Q}{\partial Z} = \varepsilon\;[{\rm erg\,cm^{-3}\,s^{-1}}] \,. \tag{12}$$

We take the opacities in the form of a power law $\varkappa = \varkappa_0 \rho^\zeta / T^\nu$ where $\zeta = \nu = 0$, $\varkappa_0 = 0.4$ cm^{2}g^{-1} if $\varkappa_{\rm T} \gg \varkappa_{\rm ff}$ and $\zeta = 1$, $\nu = 7/2$, $\varkappa_0 = 6.45 \times 10^{22}$ cm^{5}K$^{7/2}$g^{-2} if $\varkappa_{\rm ff} \gg \varkappa_{\rm T}$. Generally, in the optically thick disks the energy release can be described as a power law of temperature and density (Tayler 1980). In a sense the calculation of the disk structure resembles the calculation of stellar internal structure. In the present study two cases are considered: the energy release ε is proportional to (a) the pressure $\propto \rho T$, (b) the density ρ alone. The thermal energy release is due to the differential rotation of a viscous disk:

$$\varepsilon = -\, r\, w_{r\varphi} \frac{\partial \omega}{\partial r} = \frac{3}{2}\, \omega_{\rm K}\, w_{r\varphi}\ . \tag{13}$$

We follow Shakura (1972) and Shakura & Sunyaev (1973) in suggesting that the turbulent viscous stress tensor is parameterized by the pressure:

$$w_{r\varphi} = -\, \nu_{\rm t}\, \rho\, r \frac{\partial \omega}{\partial r} = \frac{3}{2}\, \omega_{\rm K}\, \nu_{\rm t}\, \rho\ = \alpha\, P\ , \tag{14}$$

where $\nu_{\rm t}$ is the kinematic coefficient of turbulent viscosity. The height-integrated viscous stress tensor is given by

$$W_{r\varphi}(r,t) = 2 \int\limits_0^{Z_{\rm o}} w_{r\varphi}\, {\rm d}Z\ = 3\, \omega_{\rm K} \int\limits_0^{Z_{\rm o}} \nu_{\rm t}\, \rho\, {\rm d}Z\ . \tag{15}$$

The energy emitted from the unit surface of one side of the disk is obtained by integrating (12) using (13) and (15):

$$Q_{\rm o} = \frac{1}{2}\, W_{r\varphi}(r,t)\, r \frac{\partial \omega}{\partial r} = \frac{3}{4}\, \omega_{\rm K}\, W_{r\varphi}(r,t)\ . \tag{16}$$

Above equations written for stationary accretion disks hold in a non-stationary case taking into account that the characteristic hydrostatic time of order of α/ω is shorter than the time of radial movement in the disk $r/v_r \sim (r/Z_{\rm o})^2/\alpha\omega$.

There are now various works investigating the vertical structure of the disks. For example, Nakao & Kato (1995) considered turbulent diffusion in the disk providing the variations of viscous heating and α-parameter along the height Z. The vertical structure of the disks including radiative and convective energy transfer was investigated by Meyer & Meyer-Hofmeister (1982). They investigated two types of viscosity, proportional to the gas pressure or to the total pressure. We adopt the result of Ketsaris & Shakura (1998) who proposed a new method of calculating the vertical structure of optically thick α-disks assuming power ρ– and T– dependences for the opacity and the energy release.

The dimensionless variable

$$\sigma = \frac{2\,\Sigma}{\Sigma_{\rm o}}$$

is introduced for convenient description of the problem, along with the following variables: $p = P/P_{\rm c}$, $\theta = T/T_{\rm c}$, $z = Z/Z_{\rm o}$, $j = \rho/\rho_{\rm c}$, and $q = Q/Q_{\rm o}$. The method involves the finding of the eigenvalues of the dimensionless parameters in the differential equations that describe vertical structure of the disk:

$$\begin{aligned}
&\frac{{\rm d}p}{{\rm d}\sigma} = -\Pi_1\, \Pi_2\, z\ ; \quad && \Pi_1 = \frac{\omega_{\rm K}^2\, Z_{\rm o}^2\, \mu}{\Re\, T_{\rm c}}\ ;\\
&\frac{{\rm d}z}{{\rm d}\sigma} = \Pi_2\, \frac{\theta}{p}\ ; && \Pi_2 = \frac{\Sigma_{\rm o}}{2\, Z_{\rm o}\, \rho_{\rm c}}\ ;\\
&\frac{{\rm d}q}{{\rm d}\sigma} = \Pi_3\, \theta\ ; && \Pi_3 = \frac{3}{4}\, \frac{\alpha\, \omega_{\rm K}\, \Re\, T_{\rm c}\, \Sigma_{\rm o}}{Q_{\rm o}\, \mu}\ \equiv \frac{\alpha\, \Re\, T_{\rm c}\, \Sigma_{\rm o}}{W_{r\varphi}\, \mu}\ ;\\
&\frac{{\rm d}\theta}{{\rm d}\sigma} = \Pi_4\, \frac{q\, j^\zeta}{t^{\nu+3}}\ ; && \Pi_4 = \frac{3}{32}\, \left(\frac{T_{\rm ef}}{T_{\rm c}}\right)^4\, \frac{\Sigma_{\rm o}\, \varkappa_0\, \rho_{\rm c}^\zeta}{T_{\rm c}^\nu}\ ,
\end{aligned} \tag{17}$$

using the definite boundary conditions in the disk. $T_{\rm c}$, $\rho_{\rm c}$, $P_{\rm c}$ denote the values in the equatorial plane of the disk and $Q_{\rm o} = (ac/4)\, T_{\rm ef}^4$.

After some algebraic manipulation of the right hand equations in (17) we obtain $\Sigma_{\rm o}$ written in terms of $W_{r\varphi}\, r^2$ and $\omega\, r^2$, which in view of (7) yields:

$$\begin{aligned}
D = \frac{1}{4(1-m)} \Bigg\{ &\frac{2^{6+\zeta+2\nu}\, \alpha^{8+\zeta+2\nu}}{\Pi_1^\zeta\, \Pi_2^{2\zeta}\, \Pi_3^{8+\zeta+2\nu}\, \Pi_4^2} \\
&\times \left(\frac{\Re}{\mu}\right)^{8+2\nu} \left(\frac{9\varkappa_0}{8\, a\, c}\right)^2 (GM)^{12+8\zeta} \Bigg\}^{\frac{1}{10+3\zeta+2\nu}}\ ,
\end{aligned} \tag{18}$$

where

$$m = \frac{4+2\zeta}{10+3\zeta+2\nu}\ , \qquad n = \frac{12+11\zeta-2\nu}{10+3\zeta+2\nu}\ .$$

It is worth noting that D depends on $\varkappa_0$ very weakly: to a power of $1/5$ or $1/10$. This fact is believed to reduce the effect of uncertainties in our knowledge of the real law of opacity. The combination of $\Pi_{1,2,3,4}$ in (18) varies slightly with the optical depth τ, i.e. along the radius of the disk (see Tables 1, 2). Thus, factor D in the basic equation of time-dependent accretion (6) is considered to be constant.

Specific energy dissipation $\varepsilon/\rho = \partial Q/\partial\Sigma$ is defined by the temperature variations over Z. In principle, the intensive stirring in the disk can account for the situation when the energy release per unit mass does not depend on the height Z. This refers to the case (b) mentioned above where ε is the function of density. In this situation the temperature dependence disappears in the energy production equation (third line of (17)) and $\Pi_3 = 1$.

Ketsaris & Shakura (1998) calculated the values of Π_1, Π_2, Π_3, and Π_4. Selected values of $\Pi_{1,2,3,4}$ and corresponding values of δ, in the Thomson opacity regime, and some effective optical thickness of the disk $\tau_0 = \Sigma_{\rm o}\, \varkappa_0\, \rho_{\rm c}/(2\, T_{\rm c}^{7/2})$, in the free-free regime, are shown in Tables 1, 2. For the full version of $\Pi_{1,2,3,4}$ list and discussion the reader is referred to the original paper by Ketsaris & Shakura (1998). The parameter δ was introduced by them for the sake of convenience and

Table 1. Vertical structure parameters in the Thomson opacity regime

					$\Pi_3 = 1$		
$\log\delta$	Π_1	Π_2	Π_3	Π_4	Π_1	Π_2	Π_4
4.00	6.37	0.516	1.150	0.460	6.46	0.511	0.500
3.00	5.67	0.546	1.149	0.459	5.74	0.542	0.499
2.00	4.47	0.610	1.142	0.454	4.52	0.605	0.490
1.00	2.61	0.740	1.105	0.398	2.63	0.737	0.417

Table 2. Vertical structure parameters in the free-free opacity regime

					$\Pi_3 = 1$		
$\log\tau_0$	Π_1	Π_2	Π_3	Π_4	Π_1	Π_2	Π_4
4.00	7.07	0.487	1.131	0.399	7.12	0.485	0.437
3.00	6.31	0.515	1.131	0.398	6.34	0.514	0.436
2.00	4.98	0.576	1.126	0.395	4.98	0.576	0.431
1.00	2.83	0.716	1.095	0.354	2.81	0.716	0.373

denotes the ratio of total scattering optical thickness $\varkappa_{\rm T}\,\Sigma_{\rm o}$ to that at the thermalization depth:

$$\delta = \frac{\varkappa_{\rm T}\,\Sigma_{\rm o}}{\tau_{\rm T}(\tau^*=1)}\,, \qquad \tau^* = \int\limits_{Z^*}^{Z_{\rm o}} (\varkappa_{\rm ff}\,\varkappa_{\rm T})^{1/2}\,\rho\,{\rm d}Z\,, \tag{19}$$

where τ^* is the effective optical depth (Zeldovich & Shakura 1969; Mihalas 1978).

5. Time-dependent accretion in Keplerian disk

5.1. Solutions to non-stationary Keplerian disk equation

The self-similar solutions of Eq. (6) were found by LS87. In these solutions any physical characteristic of the disk, for instance, the surface density $\Sigma_{\rm o}(r,t)$, can be presented in the form: $\Sigma_{\rm o}(r,t) = S(t)\,s(r/R(t))$, where the scales $S(t)$ and $R(t)$ depend on t in a particular way, and $s(r/R(t))$ is a universal function of one self-similar variable $\hat{\xi} = r/R(t)$ (Zeldovich & Raizer 1967). The solutions represent three stages of the non-stationary accretion on an object. The first stage is the formation of the accretion disk from some finite torus around an object. The second stage is the developing of the quasi-stationary regime of accretion, and the third – the decay of accretion when the external boundary of the disk is spreading away to infinity. LS87 obtained the self-similar solutions of type II for the first two stages and the self-similar solution of type I (Zeldovich & Raizer 1967) for the final stage (when there is conservation of the total angular momentum of the disk).

In a binary system the accretion picture has particular features. The main feature is the limitation of the outer radius. Thus, one cannot apply the LS87 solution at the third stage, that is, during the decay of accretion after the peak of the outburst. The spreading of the disk is to be confined by the tidal interactions. The tidal torque produced by a secondary star has strong radial dependence (Papaloizou & Pringle 1977). As Ichikawa & Osaki (1994) showed, the tidal effects are generally small in the accretion disk, except near to the tidal truncation radius, which is given by the last non-intersecting periodic particle orbit in the disk (Paczyński 1977). They concluded that once the disk expands to the tidal truncation radius, the tidal torques prevent the disk from expanding beyond the tidal radius.

A class of solutions of Eq. (6), which this paper focuses on, can be found on separating the variables h and t. We seek the solution in the form $F(h,t) = F(t)f(\xi)$, where $\xi = h/h_{\rm o}$, $h_{\rm o} = (GMr_{\rm out})^{1/2}$. From Eq. (4), substituting $h \equiv h_*$, it follows that

$$\dot{M}(h,t) = -2\pi f'(h/h_{\rm o})F(t)/h_{\rm o}\,. \tag{20}$$

Substitution of the product of two functions in Eq. (6) gives the time-dependent part of the solution:

$$F(t) = \left(\frac{h_{\rm o}^{n+2}}{-\lambda\, m\, D\,(t+t_0)}\right)^{1/m}. \tag{21}$$

D is the constant defined by the vertical structure of the disk (Sect. 4, Eq. (18)); λ is a negative separation constant which can be found from boundary conditions on $f(\xi)$; t_0 is an integration constant. From here on we set $t_0 = 0$ for the Thomson opacity regime. We calculate a value of t_0 for the free-free opacity regime in Sect. 6.2. Expression (21) represents asymptotic law for after-peak evolution of a real source.

The equation for $f(\xi)$ is a non-linear differential equation of second order which is a particular case of the general Emden-Fowler equation (Zaycev & Polyanin 1996):

$$\frac{d^2 f}{d\xi^2} = \lambda \xi^n f^{1-m}\,, \tag{22}$$

the solution of which we seek as a polynomial

$$f(\xi) = a_0\xi + a_1\xi^k + a_2\xi^l + \dots\,. \tag{23}$$

Substituting $f(\xi)$ into Eq. (22) we obtain for the second and the third term:

$$\begin{aligned} &k = 3+n-m, \quad a_1 = \frac{\lambda a_0^{1-m}}{k(k-1)}\,,\\ &l = 2k-1, \quad a_2 = \frac{\lambda a_0^{-m} a_1}{l(l-1)}(1-m)\,, \end{aligned} \tag{24}$$

and a_0, λ are to be defined from the boundary conditions on $f(\xi)$.

We consider the size of the disk to be maximum and invariant over the period of outburst. As the drain of angular momentum occurs in a narrow region near this truncation radius (Ichikawa & Osaki 1994), we treat the region near this radius as the δ-type channel, not considering the details of the process. In other words, the smooth behaviour of spatial factor f in the moment of viscous forces F (which increases as $\propto r^{1/2}$ in the inner parts of the disk, then flattens, reaches the maximum and drops down near $r_{\rm out}$ due to tidal torque) is analytically treated as increasing, flattening, and reaching maximum at $r_{\rm out}$, which is the end of the disk (this profile is shown in Fig. 1). Thus we propose the boundary conditions as follows:

Table 3. Summary of parameters in solutions for two opacity regimes for the Keplerian disk

	m	n	λ	a_0	a_1	a_2	k	l
$\varkappa_{\rm T} \gg \varkappa_{\rm ff}$	$2/5$	$6/5$	-3.482	1.376	-0.39	0.02	3.8	6.6
$\varkappa_{\rm ff} \gg \varkappa_{\rm T}$	$3/10$	$4/5$	-3.137	1.430	-0.46	0.03	3.5	6.0

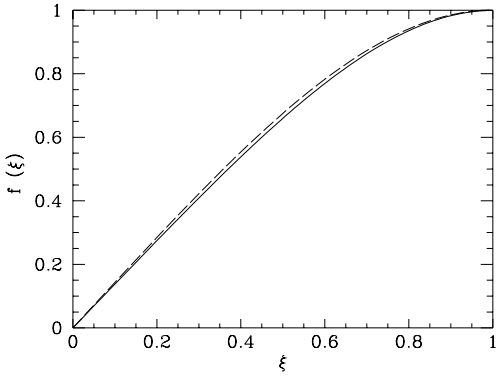

Fig. 1. The solution $f(\xi)$ in two cases: when $\varkappa_{\rm T} \gg \varkappa_{\rm ff}$ (solid line) and $\varkappa_{\rm ff} \gg \varkappa_{\rm T}$ (dashed line)

$$f(1) = 1, \quad f'(1) = 0\,. \tag{25}$$

Corresponding a_0 and λ are displayed in Table 3.

Naturally, real accretion disks have finite value of $r_{\rm in} \neq 0$, but still, in most cases, $r_{\rm in}/r_{\rm out} \ll 1$, that is equivalent to $r_{\rm in}/r_{\rm out} = 0$ in our problem from the mathematical standpoint.

Note that (21) implies a considerably *steeper* time dependence than the solution by LS87 does. The latter yields the accretion rate as a function of $t^{-19/16}$ if $\varkappa_{\rm T} \gg \varkappa_{\rm ff}$, and $t^{-5/4}$ if $\varkappa_{\rm ff} \gg \varkappa_{\rm T}$. In our case this dependence is $t^{-5/2}$ if $\varkappa_{\rm T} \gg \varkappa_{\rm ff}$, and $t^{-10/3}$ if $\varkappa_{\rm ff} \gg \varkappa_{\rm T}$. This difference is due to the non-conservation of angular momentum in the disk in our case.

The following subsections contain the explicit expressions for the physical characteristics of the disk. They are deduced from (7), (17), (18), and (21). We introduce for the mass of the central object the quantity $m_{\rm x} = M/M_\odot$.

5.2. Thomson opacity regime ($\varkappa_{\rm T} \gg \varkappa_{\rm ff}$)

Here the function $f = f(\xi) = f((r/r_{\rm out})^{1/2})$ and the values $\Pi_{1..4}$ should be taken for the Thomson opacity regime. Then we have:

$$D\ [{\rm g}^{-2/5}\,{\rm cm}^{28/5}\,{\rm s}^{-17/5}] = 2.42\times10^{39}\ \alpha^{4/5}\,m_{\rm x}^{6/5}\,\mu^{-4/5}\,\left(\Pi_3^4\,\Pi_4\right)^{-1/5}\,, \tag{26}$$

$$\Sigma_{\rm o}\ [{\rm g\,cm^{-2}}] = 3.4\times10^2\ \alpha^{-2}\,m_{\rm x}^{1/2}\,\left(\frac{\mu}{0.5}\right)^2\left(\frac{r}{r_{\rm out}}\right)^{-9/10} \times f^{3/5}\left(\frac{r_{\rm out}}{R_\odot}\right)^{3/2}\left(\frac{t}{10^{\rm d}}\right)^{-3/2}\left(\Pi_3^4\,\Pi_4\right)^{1/2}\,, \tag{27}$$

$$T_{\rm c}\ [{\rm K}] = 1.8\times10^4\,\alpha^{-1}\,m_{\rm x}^{1/2}\,\left(\frac{\mu}{0.5}\right)\left(\frac{r}{r_{\rm out}}\right)^{-11/10} f^{2/5} \times\left(\frac{r_{\rm out}}{R_\odot}\right)^{1/2}\left(\frac{t}{10^{\rm d}}\right)^{-1}\Pi_3\,, \tag{28}$$

$$\frac{z_{\rm o}}{r} = 0.03\,\alpha^{-1/2}\,m_{\rm x}^{-1/4}\left(\frac{r}{r_{\rm out}}\right)^{-1/20} \times f^{1/5}\left(\frac{r_{\rm out}}{R_\odot}\right)^{3/4}\left(\frac{t}{10^{\rm d}}\right)^{-1/2}\left(\Pi_1\,\Pi_3\right)^{1/2}\,, \tag{29}$$

$$\tau^* = 4.8\times10^2\ \alpha^{-1}\left(\frac{\mu}{0.5}\right)^{5/4}\left(\frac{r}{r_{\rm out}}\right)^{1/10} \times f^{1/10}\left(\frac{r_{\rm out}}{R_\odot}\right)^{1/2}\left(\frac{t}{10^{\rm d}}\right)^{-1/4}\left(\frac{\Pi_3^4\,\Pi_4^3}{\Pi_1\,\Pi_2^2}\right)^{1/4}\,. \tag{30}$$

τ^* is the effective optical thickness of the disk defined by the combined processes of scattering and absorption. We take approximately (cf. (19)):

$$\tau^* = \left(\frac{0.4\times6.45\times10^{22}\,\rho_{\rm c}}{T_{\rm c}^{7/2}}\right)^{1/2}\Sigma_{\rm o}\,.$$

5.3. Free-free opacity regime ($\varkappa_{\rm ff} \gg \varkappa_{\rm T}$)

Here the function f and the values $\Pi_{1..4}$ should be taken for the free-free opacity regime. The following formulae contain the constant t_0 appeared in expression (21). It was neglected in the previous subsection; here t_0 accounts for the possibility of time shifts between the solutions in the two opacity regimes. We have:

$$D\ [{\rm g}^{-3/10}\,{\rm cm}^5\,{\rm s}^{-16/5}] = 5.04\times10^{35}\,\alpha^{4/5}\,m_{\rm x}\,\mu^{-3/4}\,\left(\Pi_1^{1/2}\,\Pi_2\,\Pi_3^8\,\Pi_4\right)^{-1/10}\,, \tag{31}$$

$$\Sigma_{\rm o}\ [{\rm g\,cm^{-2}}] = 5.3\times10^2\,\alpha^{-8/3}\,m_{\rm x}^{5/6}\left(\frac{\mu}{0.5}\right)^{5/2}\left(\frac{r}{r_{\rm out}}\right)^{-11/10} f^{7/10} \times\left(\frac{r_{\rm out}}{R_\odot}\right)^{13/6}\left(\frac{t+t_0}{10^{\rm d}}\right)^{-10/3}\left(\Pi_1^{1/2}\,\Pi_2\,\Pi_3^8\,\Pi_4\right)^{1/3}, \tag{32}$$

$$T_{\rm c}\ [{\rm K}] = 3.1\times10^4\,\alpha^{-1}\,m_{\rm x}^{1/2}\left(\frac{\mu}{0.5}\right)\left(\frac{r}{r_{\rm out}}\right)^{-9/10} \times f^{3/10}\left(\frac{r_{\rm out}}{R_\odot}\right)^{1/2}\left(\frac{t+t_0}{10^{\rm d}}\right)^{-1}\Pi_3\,, \tag{33}$$

$$\frac{z_{\rm o}}{r} = 0.04\,\alpha^{-1/2}\,m_{\rm x}^{-1/4}\left(\frac{r}{r_{\rm out}}\right)^{1/20} f^{3/20} \times\left(\frac{r_{\rm out}}{R_\odot}\right)^{3/4}\left(\frac{t+t_0}{10^{\rm d}}\right)^{-1/2}(\Pi_1\,\Pi_3)^{1/2}\ , \qquad (34)$$

$$\tau = 4.5\times10^2\,\alpha^{-4/3}\,m_{\rm x}^{1/6}\left(\frac{\mu}{0.5}\right)^{3/2}\left(\frac{r}{r_{\rm out}}\right)^{-1/10} \times f^{1/5}\left(\frac{r_{\rm out}}{R_\odot}\right)^{5/6}\left(\frac{t+t_0}{10^{\rm d}}\right)^{-2/3}\left(\frac{\Pi_3^4\,\Pi_4^2}{\Pi_1^{1/2}\,\Pi_2}\right)^{1/3}\ . \qquad (35)$$

This regime is characterized by lower temperature and density, and the optical thickness of the disk is defined by the processes of free-free absorption: $\tau = 2\,\tau_0 = 6.45\times10^{22}\,\rho_{\rm c}\,T_{\rm c}^{-7/2}\,\Sigma_{\rm o}$.

6. Bolometric light curves of time-dependent standard accretion disk: power law

In order to calculate the luminosity of the disk, we assume the quasi-stationary accretion rate as it is at $r \ll r_{\rm out}$. For these most luminous parts of the disk we take $\dot{M}(t) = \dot{M}(0,t)$ given by (20). The overall emission of the disk is defined by the gravitational energy release $L = \eta\,\dot{M}(t)\,c^2$, where η is the efficiency of the process.

At early t, when the Thomson scattering is dominant, we derive that the bolometric luminosity of the disk varies as follows:

$$L_{\rm T}(t)\ [{\rm erg\,s^{-1}}] = 1.3\times10^{39}\,\alpha^{-2}\,m_{\rm x}^{1/2}\left(\frac{\eta}{0.1}\right)\left(\frac{\mu}{0.5}\right)^2 \times\left(\frac{r_{\rm out}}{R_\odot}\right)^{7/2}\left(\frac{t}{10^{\rm d}}\right)^{-5/2}\left(\Pi_3^4\,\Pi_4\right)^{1/2}\ . \qquad (36)$$

As the temperature decreases, the law of decline switches to:

$$L_{\rm ff}(t)\ [{\rm erg\,s^{-1}}] = 3.6\times10^{39}\,\alpha^{-8/3}\,m_{\rm x}^{5/6}\left(\frac{\eta}{0.1}\right)\left(\frac{\mu}{0.5}\right)^{5/2}\left(\frac{r_{\rm out}}{R_\odot}\right)^{25/6} \left(\frac{t+t_0}{10^{\rm d}}\right)^{-10/3}\left(\Pi_1^{1/2}\,\Pi_2\,\Pi_3^8\,\Pi_4\right)^{1/3}\ . \qquad (37)$$

The mass of the disk can be derived by integrating $\Sigma_{\rm o}$ over its surface:

$$M_{\rm disk,T}\ [M_\odot] = 4\times10^{-9}\,\alpha^{-2}\,m_{\rm x}^{1/2}\left(\frac{\mu}{0.5}\right)^2\left(\frac{r_{\rm out}}{R_\odot}\right)^{12/5} \times\left(\frac{t}{10^{\rm d}}\right)^{-3/2}\left(\Pi_3^4\,\Pi_4\right)^{1/2}, \qquad (38)$$

$$M_{\rm disk,ff}\ [M_\odot] = 2\times10^{-8}\,\alpha^{-8/3}\,m_{\rm x}^{5/6}\left(\frac{\mu}{0.5}\right)^{5/2}\left(\frac{r_{\rm out}}{R_\odot}\right)^{49/15} \times\left(\frac{t+t_0}{10^{\rm d}}\right)^{-7/3}\left(\Pi_1^{1/2}\,\Pi_2\,\Pi_3^8\,\Pi_4\right)^{1/3}\ . \qquad (39)$$

The constant t_0 is the same as in the previous section. These solutions give an asymptotic law for the disk *bolometric* luminosity variations. The value of t_0 will be obtained in Sect. 6.2 when we shall discuss the transition between the regimes of opacity.

We remark that the observed X-ray light curves can have *different* (most probably, steeper) law of decay. Indeed, the energy band of an X-ray detector usually covers the region harder 1 keV where the multi-color photon spectrum of the disk (having appropriate temperature) can have turnover from $-2/3$ power law into exponential fall. This turnover is expected to change its position due to variations in temperature of the disk after the burst. The narrower the observed band, the more different the observed curve could look like in comparison with the expected bolometric flux light curve. In Sect. 7 we discuss this subject in more detail.

6.1. Luminosity – accretion disk parameters dependence

It is essential to point out that in formulae (36), (37) the parameters $\alpha, \mu, m, r_{\rm out}, \Pi_{1,2,3,4}$ cannot be changed to describe how luminosity depends on them. Indeed, these expressions were found as a result of solution of differential Eq. (6) with the constant coefficient D (which depends on parameters of the disk, except η). Imagine a situation when one of these parameters, say α, quickly increases. This will not result in the decrease of the luminosity as it might seem from (36) or (37). What will happen really is that the accretion will change to another solution (during the same regime of opacity), according to the new D^*. Supposing that the mass of the disk remains constant during this transition and taking into account that the profile of $\Sigma_{\rm o}(r)$ does not change, it can be seen from (7) that F changes discontinuously and the luminosity $L \propto \dot{M} \propto F(t)$ jumps as $(\alpha^*/\alpha)^{4/(5(1-m))}$, $\alpha^* > \alpha$. The relation between the new and the old F and D, obtained from (7), gives the new term $(t+t_0^*)$ in (21):

$$\frac{t+t_0^*}{t+t_0} = \left(\frac{D}{D^*}\right)^{1/(1-m)}\ . \qquad (40)$$

Thus the increase in α gives the increase in D and, consequently, $(t+t_0^*) < (t+t_0)$ which implies a steeper light curve after the transition than before. The increase of α can be possibly provided by the enhanced role of convection in the accretion disk and will result in the brightening of the disk. This situation is displayed in the inset in Fig. 2. We note that the descending portion of the curve after the increase is uncertain if convection is involved since the disk structure modifies from that presented in Sect. 4.

6.2. Thomson opacity – free-free opacity transition

The temperature of the disk decreases with time, and eventually the free-free and free-bound opacity supersedes the Thomson one. It is possible to connect two regimes at the point (ξ, $t_{\rm tr}$), where $F_1(\xi, t_{\rm tr}) = F_2(\xi, t_{\rm tr}+t_0)$ and $\Sigma_{{\rm o},1} = \Sigma_{{\rm o},2}$ (indexes 1, 2 denote different opacity regimes) – two conditions allowing us naturally to define both $t_{\rm tr}$ and t_0:

$$t_{\rm tr} = 3.7^{\rm d}\, m_{\rm x}^{2/5}\, \alpha^{-4/5} \left(\frac{\mu}{0.5}\right)^{3/5} \left(\frac{r}{r_{\rm out}}\right)^{-4/5} \times \left(\frac{r_{\rm out}}{R_\odot}\right)^{4/5} \frac{^{\rm f}f^{12/5}}{^{\rm T}f^2} \left(\frac{^{\rm f}\Pi_1\, ^{\rm f}\Pi_2^2\, ^{\rm f}\Pi_3^{16}\, ^{\rm f}\Pi_4^2}{^{\rm T}\Pi_3^{12}\, ^{\rm T}\Pi_4^4}\right)^{1/5}, \quad (41)$$

$$t_{\rm tr} + t_0 = 6.4^{\rm d}\, m_{\rm x}^{2/5}\, \alpha^{-4/5} \left(\frac{\mu}{0.5}\right)^{3/5} \left(\frac{r}{r_{\rm out}}\right)^{-3/5} \times \left(\frac{r_{\rm out}}{R_\odot}\right)^{4/5} \frac{^{\rm f}f^{21/10}}{^{\rm T}f^{9/5}} \left(\frac{^{\rm f}\Pi_1\, ^{\rm f}\Pi_2^2\, ^{\rm f}\Pi_3^{16}\, ^{\rm f}\Pi_4^2}{^{\rm T}\Pi_3^{12}\, ^{\rm T}\Pi_4^4}\right)^{1/5}.$$

The right top indexes of $f = f(\xi)$ and $\Pi_{1,2,3,4}$ indicate the opacity regimes. As the profiles of $f(\xi) = f((r/r_{\rm out})^{1/2})$ are very close in these two regimes (see Fig. 1), and parameters $\Pi_{1,2,3,4}$ vary slightly with radius (being roughly constant in the region where the substantial mass of the disk is enclosed), the physical parameters of the disk ($\Sigma_{\rm o}(r)$, $T_{\rm c}(r)$, etc.) calculated in the two solutions are sufficiently accurately equal.

At the time $t_{\rm tr}$ the free-free absorption coefficient $\varkappa_{\rm ff} = \varkappa_0 \rho_{\rm c}^{\zeta}/T_{\rm c}^{\nu}$ calculated in the Thomson opacity regime and in the free-free opacity regime takes the form:

$$^{\rm f}\varkappa_{\rm ff}\ [{\rm cm^2 g^{-1}}] = 0.399 \left(\frac{^{\rm f}f}{^{\rm T}f}\right)^6 \frac{^{\rm f}\Pi_1^{1/2}\, ^{\rm f}\Pi_2\, ^{\rm f}\Pi_3^8\, ^{\rm f}\Pi_4}{^{\rm T}\Pi_1^{1/2}\, ^{\rm T}\Pi_2\, ^{\rm T}\Pi_3^8\, ^{\rm T}\Pi_4},$$
$$^{\rm T}\varkappa_{\rm ff}\ [{\rm cm^2 g^{-1}}] = 0.399 \left(\frac{^{\rm f}f}{^{\rm T}f}\right)^3 \frac{^{\rm f}\Pi_3^4\, ^{\rm f}\Pi_4}{^{\rm T}\Pi_3^4\, ^{\rm T}\Pi_4}. \quad (42)$$

The closeness of $\varkappa_{\rm ff}$ to $\varkappa_{\rm T} = 0.4\,{\rm cm^2 g^{-1}}$ confirms the reliability of our calculations and yields the smoothness of the transition.

Fig. 2 represents the bolometric light curve of the disk for $\alpha = 0.3$, $m_{\rm x} = 3$. Hereafter we substitute $\Pi_{1,2,3,4}$ with their typical values in a self-consistent way. The transfer between Thomson and free-free regimes begins at the moment $r/r_{\rm out} = \xi^2 = 1$, $t \approx 8^{\rm d}(m_{\rm x}/3)^{2/5}\,\alpha^{-4/5}\,(\mu/0.5)^{3/5}\,(r_{\rm out}/R_\odot)^{4/5}$ – arrow A at $21^{\rm d}$ in Fig. 2. We intersect the curves at

$$r/r_{\rm out} = 0.5\,,$$
$$t = t_{\rm tr} \approx 13^{\rm d}(m_{\rm x}/3)^{2/5}\,\alpha^{-4/5}\,(\mu/0.5)^{3/5}\,(r_{\rm out}/R_\odot)^{4/5}\,,$$

what corresponds to $t_{\rm tr} \approx 34^{\rm d}$ and $t_0 \approx 17^{\rm d}$ for $\alpha = 0.3$ (left small arrow). We call $t_{\rm tr}$ "moment of transition". The transition ends at the time $t \approx 21^{\rm d}(m_{\rm x}/3)^{2/5}\,\alpha^{-4/5}\,(\mu/0.5)^{3/5}\,(r_{\rm out}/R_\odot)^{4/5}$ when the solutions match at $r = 0.25\,r_{\rm out}$ – arrow B at $55^{\rm d}$ in Fig. 2.

This picture is reliable and useful, even though it implies the existence of two separate regimes, which is evidently not quite true. Indeed, at any epoch the inner part of the disk would be scattering dominated, the lower the accretion rate, the smaller this part. Obtaining of an exact solution needs consideration of combined free-free and Thomson opacity of the gas.

There is some t which corresponds to the Eddington limit $L_{\rm Edd} \approx 1.3 \times 10^{38}\, m_{\rm x}$ erg s^{-1}. This means that the real source evolution could be described in our model only at later t. Thus, generally speaking, the solution before this moment appears inapplicable. As seen in Fig. 2, the applicable part of the solution

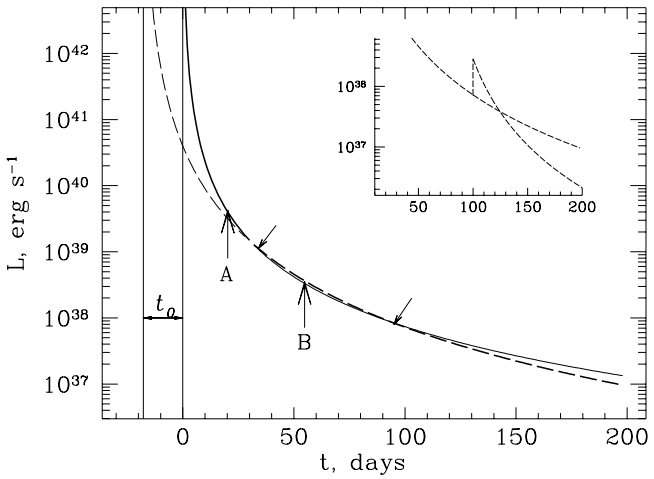

Fig. 2. Bolometric luminosity $L_{\rm T}$ and $L_{\rm ff}$ calculated for parameters: $m_{\rm x} = 3$, $\alpha = 0.3$, $\mu = 0.5$, $r_{\rm out} = R_\odot$. Shown are the solution in Thomson opacity regime (solid line) and in the free-free opacity regime (dashed line). Their bold parts represent the resulting light curve of the disk. Small arrows mark two intersections when $F_1(\xi, t) = F_2(\xi, t + t_0)$. The inset illustrates the case of increase of α from 0.3 to 1

belongs almost entirely to the free-free opacity regime (the bold dashed line).

The second intersection of the curves in Fig. 2 at $t \approx 95^{\rm d}$ (right small arrow) corresponds to the other intersection of functions $F_1(\xi, t) = F_2(\xi, t + t_0)$, meanwhile the physical parameters of the disk calculated using formulae (26)–(35) are different. Thus the disk is at the same (free-free) opacity regime as before.

When $T_{\rm c}$ decreases to the value $\sim 10^4$ K, the convection (which presumably appeares in the zones of partial ionization) starts to influence the disk's structure, and the diffusive type of radiation transfer, which we use, is no longer valid. For $m_{\rm x} = 3$ and $\alpha = 0.3$ this happens at $t \approx 190^{\rm d}$: $t + t_0 \approx 32^{\rm d}\, m_{\rm x}^{1/2}\,\alpha^{-1}\,(\mu/0.5)\,(r_{\rm out}/R_\odot)^{1/2}\,(r/r_{\rm out})^{-9/10}\, ^{\rm f}f^{3/10}\, ^{\rm f}\Pi_3$. For investigation of the disk evolution on larger time-scales see e.g. Cannizzo et al. (1995), Cannizzo (1998), Kim et al. (1999).

7. Observed light curves

As we mentioned in Sect. 6, the observed light curves can have a slope of decline which is *different* from that of the bolometric light curves due to particular spectral distribution. In this section we are going to illustrate this suggestion assuming the simplest spectral distribution of the disk emission. To calculate the spectra, one can assume the quasi-stationary accretion rate in the inner parts of the disk because the $\dot{M}$ variation is small there ($\dot{M} \propto f'(\xi)$, see Fig. 1). The outer parts of the disk, where accretion rate varies significantly, contributes to the low-frequency band of the spectrum. We discuss the X-ray band and the most luminous parts of the disk and, thus, we take $\dot{M}(t) = \dot{M}(0, t)$ given by (20).

Provided each ring in the disk emits as a black body, the temperature of the ring can be found as follows:

$$\sigma_{\rm SB}\, T^4 = -\frac{1}{2}\, W_{r\varphi}\, r\, \frac{{\rm d}\,\omega_{\rm K}}{{\rm d}r} = \frac{3}{4}\,\omega_{\rm K}\, W_{r\varphi}\,, \quad (43)$$

where $\sigma_{\rm SB} = 5.67 \times 10^{-5}$ erg cm^{-2}s^{-1}K^{-4} is the Stephan-Boltzmann constant. Then

$$T(r,t) = \left(\frac{3\,G\,M\,\dot{M}(t)}{8\,\pi\,\sigma_{\rm SB}\,r^3} \left\{ 1 - \sqrt{\frac{r_{in}}{r}} \right\} \right)^{1/4} . \qquad (44)$$

In the last expression the stationary solution for $W_{r\varphi}$ is taken. The black-body approximation is satisfactory if $\varkappa_{\rm ff} \gg \varkappa_{\rm T}$. Then the outgoing spectrum is the sum of Planckian contributions of each ring of the disk and has the characteristic $1/3$ slope for photon energies $\ll kT_{\max}$, where $T_{\max}$ is the maximum effective temperature of the disk (Lynden-Bell 1969). However, if the Thomson scattering on free electrons contributes substantially to the opacity, the outgoing spectrum is modified (Shakura & Sunyaev 1973). See e.g. Ross & Fabian (1996) for investigation of spectral forms of accretion disks in low-mass X-ray binaries.

The light curve is simulated by integrating at each t the spectral density

$$I_\nu = \frac{4\,\pi^2\,h_{\rm P}\,\nu^3}{c^2} \int\limits_{r_{\rm in}}^{r_{\rm out}} \frac{r\,{\rm d}r}{\exp\left(h_{\rm P}\,\nu / k\,T(r,t)\right) - 1} \qquad (45)$$

over the specific frequency range using (20) and (44), where $h_{\rm P} = 6.626 \times 10^{-27}$ erg s is the Planck constant. The numerical factor in (45) corresponds to the luminosity outgoing from *one* side of the disk.

Explaining the observed faster-than-power decay of outbursts in soft X-ray transients, one must take into account the specificity of the energetic band of the detector. Naturally, the observed slope of the curve depends on width and location of the observing interval. The narrower this band, the more different the observed curve could look like in comparison with the expected bolometric light curve. Of course, this difference also reflects the spectral distribution of energy coming from the source.

We show here how the slope of the curve changes in the simplest case of multi-color black body disk spectrum according to which spectral range is observed. Following (45) we calculate I_ν and integrate it over three energy ranges: 3–6 keV, 1–20 keV and that one in which practically all energy is emitted. Fig. 3 shows the photon flux variations in two X-ray energy ranges (those of *Ariel 5* and *EXOSAT* or *Ginga* observatories) and the bolometric flux variation for the face-on disk at an arbitrary distance of 1 kpc. The vertical line marks the time after which bolometric luminosity of the disk's one side is less than $L_{\rm Edd}$.

One can see an almost linear trend of the X-ray flux when bolometric luminosity is under the Eddington limit (to the right of the vertical line in Fig. 3), especially in intervals of $\sim 50^{\rm d}$. The decline becomes closer to the exponential one with time. The slope of the curve depends on α, m, $r_{\rm out}$, and other parameters. For the same parameters as in Fig. 2, the e-folding time falls in the range 20–30 days for the lower curve (3–6 keV). For instance, smaller α will result in less steep decline.

The natural explanation of such a result is the following: because the spectral shape of the disk emission has Wien-form (exponential fall-off) at the considered X-ray ranges, the law of variation of X-ray flux is roughly proportional to $\exp\left(-h_{\rm P}\,\nu / k\,T^{\rm eff}(t)\right)$. In the free-free regime of opacity we have $T^{\rm eff}(t) \propto L_{\rm ff}^{1/4}(t) \propto \dot{M}(t)^{1/4} \propto t^{-10/12}$ (see Sect. 5.1). Consequently, the observed X-ray flux varies like $\exp\left(-t^{5/6}\right)$, which is quite close to exponential behavior. We restrict ourselves to this brief and general discourse, as a detailed application of our model to observed sources is not a goal of this paper.

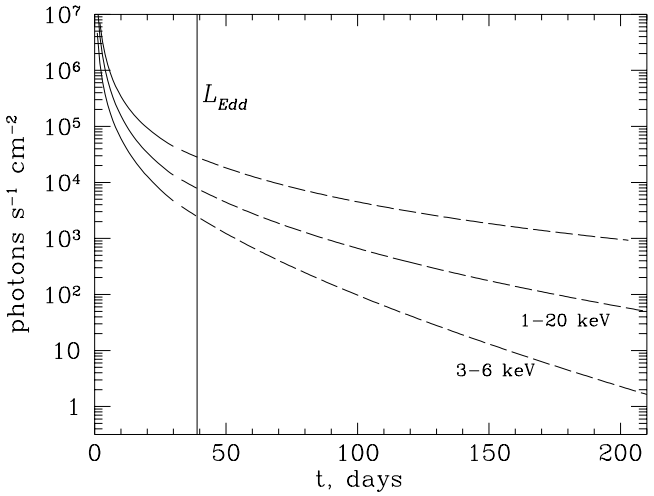

Fig. 3. The flux from one side of accretion disk at 1 kpc for parameters: $m_{\rm x} = 3$, $\alpha = 0.3$, $\mu = 0.5$, $r_{\rm out} = R_\odot$. The curves show the bolometric flux (upper curve), the 1–20 keV flux (middle curve) and the 3–6 keV flux (lower curve) during the Thomson opacity regime (solid parts) and the free-free opacity regime (dashed parts)

8. Viscous evolution of advective disk

As we know, the structure of an accretion disk in the vertical direction, the relation between the viscous tensor and the surface density in particular, defines the type of its temporal evolution. In advective disks, which are the low-radiative accretion flows, the relations between their characteristic physical parameters differ significantly from those in standard disks. In this section, we discuss the results of Sect. 2 as applied to the disks which radial structure was presented by Spruit et al. (1987) and Narayan & Yi (1994, 1995, hereafter NY).

The viscous stress and the surface density are related through the kinematic coefficient of turbulent viscosity. Integrating the component of viscous stress tensor one obtains (cf. (14) and (15)):

$$W_{r\varphi}(r,t) = 2 \int\limits_0^{z_{\rm o}} w_{r\varphi}\,{\rm d}z = -2 \int\limits_0^{z_{\rm o}} \rho\nu_{\rm t}\,\frac{\partial\omega}{\partial r}\,r\,{\rm d}z$$
$$= -\frac{\partial\omega}{\partial r}\,r\,\Sigma_{\rm o}\,\bar{\nu}_{\rm t}\,, \qquad (46)$$

where $\bar{\nu}_{\rm t}$ is the averaged kinematic coefficient of turbulent viscosity. Then the relation between $\Sigma_{\rm o}(h,t)$ and $F = W_{r\varphi}\,r^2$ is given by

$$F = \left(2\,\frac{h_*}{h} - \frac{1}{2}\,\left[\frac{\partial h_*}{\partial h}\right] \right)\, h\,\Sigma_{\rm o}\,\bar{\nu}_{\rm t}\ . \qquad (47)$$

Recall that h_* is the real specific angular momentum and h is the Keplerian one. It can be seen that $\bar{\nu}_{\rm t}(h,t)$ and $h_*(t)$ define what class of solutions Eq. (5) will have.

If one adopts for the structure of advection-dominated accretion flow (ADAF) the self-similar solution by NY, it can be easily inferred that such disks exhibit the exponential with time behaviour. The solution of NY is given by:

$$v_r = -c_1\,\omega_{\rm K}\,r\ , \qquad \omega = c_2\,\omega_{\rm K}\ , \qquad a_{\rm s}^2 = c_3\,\omega_{\rm K}^2\,r^2\ . \qquad (48)$$

Expressing $\Sigma_{\rm o}$ in the basic Eq. (5) in terms of F, we obtain from (47) and (48):

$$\frac{\partial F}{\partial t} = \frac{3}{4}\,\bar{\nu}_{\rm t}\,\frac{(GM)^2}{h^2}\,\frac{\partial^2 F}{\partial h^2}\ . \qquad (49)$$

Solution (48) enables deriving the relation between $\bar{\nu}_{\rm t}$ and $h = \omega_{\rm K}\,r^2$ using the α prescription of viscosity:

$$w_{r\varphi} = -\,\bar{\nu}_{\rm t}\,\rho\,r\,\frac{\partial \omega}{\partial r} = \frac{3}{2}\,\bar{\nu}_{\rm t}\,\rho\,c_2\,\omega_{\rm K} = \alpha\,\rho\,a_{\rm s}^2\ , \qquad (50)$$

where $a_{\rm s}$ is the isothermal sound speed. Thus $\bar{\nu}_{\rm t}$ is a function of radius alone,

$$\frac{\bar{\nu}_{\rm t}}{h} = \frac{2\,\alpha\,a_{\rm s}^2}{3\,c_2\omega_{\rm K}}\,\frac{1}{\omega_{\rm K}\,r^2} \;=\; \frac{2}{3}\,\frac{c_3}{c_2}\,\alpha\ , \qquad (51)$$

and Eq. (49) can be rewritten in the form:

$$\frac{\partial F}{\partial t} = \frac{D_{\rm a}}{h}\,\frac{\partial^2 F}{\partial h^2}\ , \qquad D_{\rm a} = \frac{\alpha\,c_3}{2\,c_2}\,(GM)^2\ . \qquad (52)$$

Solution to (52) is sought as a product of two functions $f(\xi)$ and $F(t)$, with $\xi = h/h_{\rm o}$, $h_{\rm o}$ being some value of h:

$$F(t) = F^{\rm o}\,\exp\left(\lambda\,D_{\rm a}\,t/h_{\rm o}^3\right)\ , \qquad (53)$$

$$\frac{d^2 f}{d\xi^2} = \lambda\,\xi\,f\ . \qquad (54)$$

The exponential temporal behaviour of NY flow is evident. Generally speaking, any disk possessing such properties of $\bar{\nu}_{\rm t}$ as constancy in time would have such exponential behaviour because its evolution would be described by a linear equation (like (52)).

The question is, would the confined NY disk keep such properties or it would not. The fact is that NY solution describes the infinite disk. Either the boundary conditions destroy the linearity of (52) or just the characteristic decay time changes, this problem requires further accurate numerical investigation. For instance, Narayan et al. (1997) calculated numerically the global structure of stationary advection-dominated flow with consistent boundary conditions; they noted that although the self-similar solution (48) makes significant errors close to the boundaries, it gives the reasonable description of the overall properties of the flow.

Further we assume that exponential trend of solution persists. Generally speaking, the equation determining $f(\xi)$ will differ from (54). This difference may be not very significant. One can see that Eq. (54) is a particular case of (22) where $n = 1$ and $m = 0$ and, hence, the solution can be found according to (24) and (23). Besides, the solution of (54) can be found in terms of Airy functions (Bessel functions of order $1/3$).

The accretion rate evolves with time as follows (cf. (20) and (53)):

$$\dot{M} \propto \exp\left(\lambda\,D_{\rm a}\,t/h_{\rm o}^3\right)\ . \qquad (55)$$

The value of accretion rate can be determined if an initial condition is imposed at some t. Mahadevan (1997) showed that ADAF luminosity $\propto \dot{M}^2$ or $\propto \dot{M}$ according to whether the electron heating is dominated by the Coulomb interactions or by the viscous friction. Subsequently, the luminosity has an exponential decay too.

We can estimate the characteristic time of evolution of such flow. It can be obtained from (55). Let us compare the diffusion time $t_{\rm ev} \simeq r^2/\bar{\nu}_{\rm t}$ with the corresponding orbital period $2\pi/\omega$. Since $\bar{\nu}_{\rm t} \simeq \alpha\,a_{\rm s}^2/\omega$, with (48) we have:

$$\frac{t_{\rm ev}}{t_{\rm orb}} \;=\; \frac{1}{\alpha}\,\frac{c_2^2}{2\,\pi\,c_3} = \frac{1}{2\,\pi\,\alpha}\,\frac{5/3-\gamma}{(\gamma-1)\,f_{\rm a}}\ . \qquad (56)$$

We use the expressions for c_2 and c_3 from NY. Here γ is the ratio of specific heats; $f_{\rm a}$ measures the efficiency of radiative cooling. In the limit of no radiative cooling, we have $f_{\rm a} = 1$ while in the opposite limit of very efficient cooling $f_{\rm a} = 0$. NY solution is degenerate if $\gamma = 5/3$ because the angular velocity of the flow is zero in this case.

We can see that the time-dependent advection-dominated disk is quickly depleted if α is not small. For example, consider the light curves of X-ray novae which have the exponential decay time scales $\sim 30^{\rm d}$. To obtain $t_{\rm ev}$ of such order, α should be $\sim 10^{-2}$. However, the advection-dominated solution ceases to exist if the accretion rate is greater than the critical value $\dot{M}_{\rm crit} \sim \alpha^2\,\dot{M}_{\rm Edd}$ (Narayan & Yi 1995, Mahadevan 1997), where $\dot{M}_{\rm Edd} = L_{\rm Edd}\,(\eta/0.1)^{-1}\,c^{-2} = 1.39\times10^{18}\,m_{\rm x}$. Hence, $\alpha \sim 10^{-2}$ yields the critical accretion rate $\dot{M}_{\rm crit} \sim 10^{14}\,m_{\rm x}$ g s^{-1} $\sim 10^{-4}\dot{M}_{\rm Edd}$.

9. Discussion and conclusion

In this work, we presented the analytical solutions to time-dependent accretion in binary systems. During an outburst we propose the specific external boundary conditions on a disk confined due to tidal interactions. For two opacity regimes the full analytical time-dependent solutions for the Keplerian disk are obtained and an *asymptotic* light curve is calculated with smooth transition between opacity regimes. During the decline phase accretion disks around black holes appear to be dominated by the free-free and free-bound opacity in order to comply with the Eddington limit on luminosity. This phase is characterized by the power-law decay of accretion rate $\propto t^{-10/3}$. It is shown that the decay time scale depends on the real energetic band of detector (Fig. 3).

The results obtained in this work can be applied to the accreting systems having variable emission of flare type if emission

is essentially due to the fully ionized accretion disk around a black hole, or a neutron star, or a white dwarf.

Narayan & Yi (1994) accretion flows are shown to undergo exponential decays if the disk has infinite size. This notable result probably persists even when the advective disk is in a binary system. The latter suggestion is to be thoroughly considered in the accurate numerical investigation. If this is the case, the abrupt steep falls observed in several X-ray novae (Tanaka & Shibazaki 1996) in the last phase of the decay, at luminosity levels $\lesssim 10^{36}$ erg s^{-1}, can be interpreted in terms of quickly depleting ADAF (Sect. 8) with relevant values of $\alpha \sim 10^{-1}$.

Using the results of this work, we can explain the general features of X-ray novae light curves in the early phase. Typical XN outburst light curves (see Tanaka & Shibazaki 1996; Chen at al. 1997 for a review) show quasi-exponential decay. To date several approaches have been used to account for XN features. The exponential decays were obtained in the framework of disk instability model (Cannizzo et al. 1995; Vishniac 1997; Cannizzo 1998) in which the large time-scale evolution of the disk is considered. Mineshige et al. (1993) argued that the exponential decays in XN can be reproduced if the mass and the angular momentum are efficiently removed from the inner portions of the disk at a constant rate, or wind mass loss or enhanced tidal dissipation could be substantial. King & Ritter (1998) took into account the irradiation of the disk by the central X-ray source and obtained the characteristic XN light curves.

We suggest an alternative reason to explain this remarkable feature, at least during the early stages of the outburst when the disk is fully ionized. Nearly exponential X-ray decays $\propto \exp(-t^{5/6})$ are obtained taking into account the fact that the X-ray light curves are observed in the energetic range where the spectrum of the disk has Wien-form. Black hole XN spectra typically are composed of an ultrasoft component and a hard power-law component (e.g. Tanaka 1992; Tanaka & Shibazaki 1996). At the first stages after outburst the ultrasoft component dominates and can be represented by a multicolor blackbody disk (Tanaka 1992). This component has an exponential fall-off, a decisive factor to produce observed exponential trends. The observed characteristic times can be obtained within reasonable intervals of parameters (Fig. 3, Sect. 7).

The secondary peak commonly observed in XN can be qualitatively analytically produced by certain reconstruction of viscosity mechanisms and corresponding increase of α (Sect. 6.1). Possible mechanisms of reflares involving irradiation effects were investigated by Kim et al. (1994), Mineshige (1994), King & Ritter (1998) (see, however, Cannizzo 1998).

Of course, the accretion disk spectrum represents only one contribution to the total observed spectrum of the source. The corona around the disk is probably responsible for the other spectral components. In addition, taking into consideration the irradiation of the outer parts of the disk would affect evolution of the disk (see, e.g. King & Ritter 1998; Kim et al. 1999). Kim et al. (1999) constructed an optical light curve of a XN and found the direct irradiation of the disk by the inner layers to have only a small effect on the outer disk because of shadowing. The indirect irradiation (from a corona or a chromosphere above the disk) is found to affect the light curve more strongly. We suggest that the irradiation of the twisted warped disk could also result in important heating of the outer layers. Further investigation and applications to observed sources will be the basis of our future work.

Acknowledgements. We are grateful to the anonymous referee for helpful arguments and comments. This work is partially supported by the RFBR grant 98–02–16801 and the program 'Universitety Rossii' (grant 5559) of the Ministry of Teaching and Professional Education, Russia. GVL is thankful to RFBR project 'Molodye uchenye Rossii' of 1999.

References

Cannizzo J.K., Chen W., Livio M., 1995, ApJ 454, 880
Cannizzo J.K., 1998, ApJ 494, 366
Chen W., Shrader C.R., Livio M., 1997, ApJ 491, 312
Filipov L.G., 1984, Adv. Space Res. 3, 305
Ichikawa S., Osaki Y., 1994, PASJ 46, 621
Kato S., Fukue J., Mineshige S., 1998, Black-hole Accretion Disks. Kyoto University Press, Japan
Ketsaris N.A., Shakura N.I., 1998, Astronomical and Astrophysical Transactions 15, 193
Kim S.-W., Wheeler J.C., Mineshige S., 1994, American Astr. Soc. 185, 1109
Kim S.-W., Wheeler J.C., Mineshige S., 1999, PASJ 51, 1999
King A.R., Ritter H., 1998, MNRAS 293, L42
Lüst R., 1952, Naturforsch. 7a, 87
Lynden-Bell D., 1969, Nat 233, 690
Lynden-Bell D., Pringle J.E., 1974, MNRAS 168, 603
Lyubarskii Yu.E., Shakura N.I., 1987, SvA 13, 386
Meyer F., Meyer-Hofmeister E., 1982, A&A 106, 34
Mahadevan R., 1997, ApJ 477, 585
Mihalas D., 1978, In: Freeman W.H. (ed.) Stellar Atmospheres. San Francisco
Mineshige S., Yamasaki T., Ishizaka C., 1993, PASJ 45, 707
Mineshige S., 1994, ApJ 431, L99
Nakao Y., Kato S., 1995, PASJ 47, 451
Narayan R., Yi I., 1994, ApJ 428, L13
Narayan R., Yi I., 1995, ApJ 452, 710
Narayan R., Kato S., Honma F., 1997, ApJ 476, 49
Ogilvie G.I., 1999, MNRAS 306, L90
Paczyński B., 1977, ApJ 216, 822
Papaloizou J., Pringle J.E., 1977, MNRAS 181, 441
Ross R.R., Fabian A.C., 1996, MNRAS 281, 637
Shakura N.I., 1972, AZh 49, 921
Shakura N.I., Sunyaev R.A., 1973, A&A 24, 337
Spruit H.C., Matsuda T., Inoue M., Sawada K., 1987, MNRAS 229, 517
Tanaka Y., 1992, In: Makino F., Nagase F. (eds.) Ginga Memorial Symp., ISAS, p. 19
Tanaka Y., Shibazaki N., 1996, ARA&A 34, 607
Tayler R.J., 1980, MNRAS 191, 135
Vishniac E.T., 1997, ApJ 482, 414
Weizsäcker C.F., 1948, Z. Naturforsch. 3a, 524
Zaycev V.F., Polyanin A.D., 1996, Handbook of Partial Differential Equations. Moscow
Zeldovich Ya.B., Raizer Yu.P., 1967, Physics of Shock Waves and High-Temperature Hydrodynamic Phenomena. Academic Press, New York
Zeldovich Ya.B., Shakura N.I., 1969, AZh 46, 225